



## Light-trapping Properties of a Diffractive Honeycomb Structure in Silicon

Journal:	<i>Journal of Photovoltaics</i>
Manuscript ID:	JPV-2012-11-0334-R
Manuscript Type:	Regular
Date Submitted by the Author:	12-Nov-2012
Complete List of Authors:	Thorstensen, Jostein; Institute for Energy Technology, Department for Solar Energy; University of Oslo, Department of Physics Gjessing, Jo; Institute for Energy Technology, Department for Solar Energy; University of Oslo, Department of Physics Marstein, Erik; Institute for Energy Technology, Department for Solar Energy Foss, Sean Erik; Institute for Energy Technology, Department for Solar Energy
Area of Expertise:	PV Si Defect Passivation and Advanced Optics, Laser applications

SCHOLARONE™  
Manuscripts

Only

# Light-trapping Properties of a Diffractive Honeycomb Structure in Silicon

Jostein Thorstensen, Jo Gjessing, Erik Stensrud Marstein and Sean Erik Foss

**Abstract**— Thinner solar cells will reduce material costs, but require light trapping for efficient optical absorption. We have already reported development of a method for fabrication of diffractive structures on solar cells. In this paper, we create these structures on wafers with a thickness between 21  $\mu\text{m}$  and 115  $\mu\text{m}$ , and present measurements on the light-trapping properties of these structures. These properties are compared with those of random pyramid textures, isotropic textures, and a polished sample. We divide contributions into optical loss into front surface reflectance, escape light and parasitic absorption in the rear reflector. We find that the light-trapping performance of our diffractive structure lies between that of the planar and the random pyramid textured reference samples. Our processing method, however, causes virtually no thinning of the wafer, is independent of crystal orientation and does not require seeding from e.g. saw damage, making it well suited for application to thin silicon wafers.

**Index Terms**—Laser processing, Light trapping, Optical characterization, Silicon solar cells.

## I. BACKGROUND

$P^{\text{V}}$  is rapidly moving towards direct competitiveness with alternative energy sources, and grid parity is already reached in some locations [1]. One way to continue this trend is to reduce silicon consumption. This can be achieved by using thinner wafers, and/or by moving to kerf-less wafering technologies capable of delivering cells with a thickness of 20  $\mu\text{m}$  or below. Such methods have been presented by several authors, being based on proton implantation [2], etching and layer transfer [3], exfoliation [4] or epitaxial growth [5]. Some of these methods are currently commercially available. Thin cells also reduce the requirements on material bulk quality and allow higher open circuit voltage ( $V_{\text{oc}}$ ). However, in such thin

Manuscript received November 9, 2012. This work has been funded by the Research Council of Norway through the project “Thin and highly efficient silicon-based solar cells incorporating nanostructures”, project number 181884/S10, and by “The Norwegian Research Centre for Solar Cell Technology” project number 193829, a Centre for Environment-friendly Energy Research co-sponsored by the Norwegian Research Council and research and industry partners in Norway.

J. Thorstensen, J. Gjessing, E. S. Marstein and S. E. Foss are with the Institute for Energy Technology, Department of Solar Energy, P. O. Box 40, 2027 Kjeller, Norway

J. Thorstensen and J. Gjessing are also with the University of Oslo, Department of Physics, P. O. Box 1048 Blindern, 0316 Oslo, Norway

J. Thorstensen is the corresponding author (phone: +47 63806445; fax: +47 63812905; e-mail: jostein.thorstensen@ife.no).

cells, a significant part of the sunlight may be lost due to insufficient absorption in the near infrared. In order to overcome this problem and avoid excessive efficiency loss, an efficient light-trapping scheme must be applied.

For mono-crystalline silicon with a  $\langle 100 \rangle$  orientation, the industry standard for light trapping structures today is the random pyramid texture, an excellent light trapping texture created by anisotropic alkaline etching. However, neither for the multi-crystalline silicon (mc-silicon) nor for the  $\langle 111 \rangle$ -oriented wafers typically created by proton implantation [2], can the random pyramid texture be applied, and one is left with the far less efficient isotropic acidic etch for surface texturing. Furthermore, both of the above mentioned texturing processes cause significant thinning of the wafer, and seeding for the textures may prove a challenge for wafers with no saw damage [6]. These textures may as such be unsuitable for thin cells altogether.

Diffractive structures are periodic structures with periodicity in the range of the wavelength of light. These structures can be optimized to trap light by tuning their dimensions such as periodicity and structure height [7]. However, fabrication of such structures remains an obstacle for commercial use. Only a few fabrication methods for creation of diffractive structures suitable for thin silicon solar cells have been shown, among which are hot embossing [8] and nanoimprint- or interference lithography [9]–[11] using reactive ion-etching and plasma-etching. In this work we investigate a different route for fabrication of sub-micrometer sized diffractive structures in thin Si wafers based on wet etching.

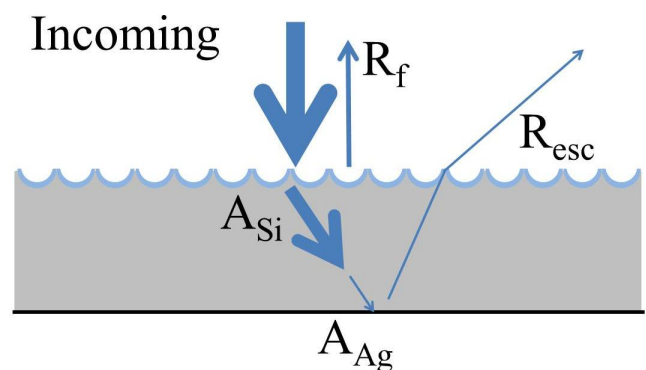


Fig. 1. Schematic figure showing the various absorption and loss mechanisms. (Not to scale.) The silicon wafer is shown in grey, the rear reflector in black and the anti-reflection coating in blue. Indicated are: The incoming sunlight, the front reflectance ( $R_f$ ), the silicon absorption ( $A_{Si}$ ), the parasitic absorption in the rear mirror ( $A_{Ag}$ ) and the escape light ( $R_{esc}$ ).

> REPLACE THIS LINE WITH YOUR PAPER IDENTIFICATION NUMBER (DOUBLE-CLICK HERE TO EDIT) <

2

In previous work [12], we present a method for fabrication of a hexagonal dimple structure suitable for a diffractive rear reflector. Using isotropic wet-etching, the process is suitable both for multi-crystalline silicon and for  $\langle 111 \rangle$  silicon. In this article, we investigate the optical properties of these structures, deposited on silicon wafers with a thickness of 21 – 115  $\mu\text{m}$ . For reference we use Si wafers with random pyramids, with isotropic texture resulting from acidic etching, and a planar wafer. We investigate the optical absorption properties of the textures, and examine sources of loss. As schematically shown in Fig. 1, we divide the sources of loss into primary reflectance ( $R_f$ ), escape light ( $R_{esc}$ ) and absorption in the rear mirror ( $A_{Ag}$ ). The primary reflectance consists of the light that is reflected off the front surface and, hence, does not enter the wafer. This contribution will, in general, be higher for planar than for textured front surfaces. Escape light refers to the part of the light that has entered the wafer, but is not absorbed and escapes through the front surface. This contribution is an indication of the light-trapping properties of the texture. Finally, the rear reflector may absorb a fraction of the light that reaches the rear surface. This contribution will depend on the type of metal used, and on the geometry of the reflector. Generally, a textured metal surface will have a larger absorption than a planar rear reflector [13]. In order to investigate the optical properties closer, we shall use our texture either as a front side texture or as a rear side texture.

## II. EXPERIMENTAL

### A. Texturing process

Our method for creating honeycomb structures on silicon is schematically represented in Fig. 2. Details on the process may be found elsewhere [12],[14]. The spheres have a diameter of 0.96  $\mu\text{m}$ , close to the predicted optimum for a rear-side diffractive grating on 20  $\mu\text{m}$  thick Si wafers [7], [15]. In order to be able to cover the entire surface uniformly, we have applied a square top-hat intensity profile, by inserting a beam shaping element before the focusing lens. The size of the laser spot is approx. 150x150  $\mu\text{m}$ . The texture is characterized using Scanning Electron Microscopy (SEM).

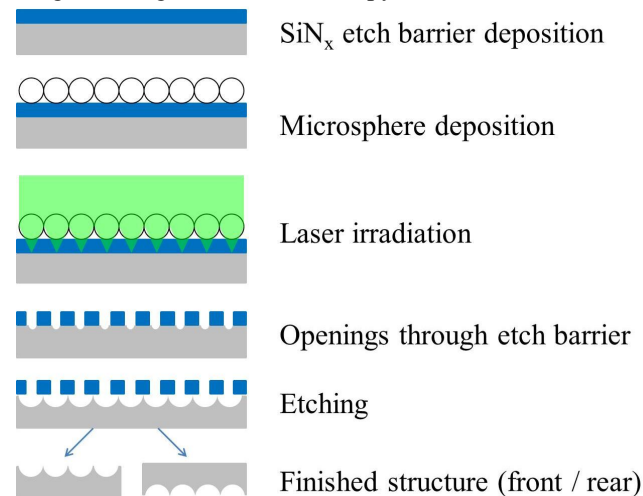


Fig. 2. Schematic representation of the texturing process.

After creating the textures, a SiN<sub>x</sub> anti-reflection coating (ARC) is deposited on the front surface of the wafer, and a 200 nm thick PECVD-SiO<sub>x</sub> spacing layer is deposited on the rear surface. For the rear side reflector, we apply two different silver (Ag) reflectors. The first Ag reflector is a detached planar reflector, which is evaporated onto a microscope slide and placed at the rear of the wafer. The second Ag reflector is a reflector which is evaporated onto the rear of the wafer (onto the SiO<sub>x</sub>). This reflector will follow the shape of the wafer and spacing layer.

For comparison of the properties of the textures, we also prepare reference textures; random pyramid textures and isotropic textured wafers are prepared from diamond-sawed wafers (both sides are textured). The random pyramids are etched in a 1 % (wt) KOH, 4 % (wt) isopropanol solution at 78 °C for 40 min. The isotropic etched samples are etched in a CP5-solution (10:5:2, HNO<sub>3</sub>:CH<sub>3</sub>COOH:HF) at 20°C for 70 and 180 seconds. A double-side polished wafer is also used as reference. Each of the reference structures exhibit the same SiN<sub>x</sub> ARC and SiO<sub>x</sub> spacing layer as the dimple structures.

### B. Optical characterization and calculation of optical losses

We measure the reflectance of the samples with an integrating sphere in a center mount configuration, i.e. with the samples inside the integrating sphere (type Labsphere RTC-060-SF). Reflectance is first measured with detached rear reflectors, and then measured again after we deposit Ag on the rear side of the samples. With zero transmission the spectral absorption,  $A_{meas}(\lambda)$ , is unity minus the measured reflectance, i.e.  $1 - R_{meas}(\lambda)$ .

For wavelengths,  $\lambda$ , above the band gap of Si (1200-1400 nm) the absorption curves tend to stabilize at absorption levels typically between a few percent and up towards 20 percent, as seen in Fig. 4. We use this plateau value to separate Ag absorption from Si absorption. Hence, we implicitly assume a constant rear reflectivity in the spectral range where the Si is sufficiently transparent so that light may be absorbed in the Ag rear reflector, i.e. about 800-1400 nm. This assumption is motivated by the occurrence of a plateau above the Si band gap together with the fact that Ag reflectivity is quite flat in this spectral range.

We estimate the front side reflectance,  $R_f(\lambda)$ , by linear extrapolation of the measured reflectance at shorter wavelengths, where the contribution from rear side reflectance is negligible. The method of extrapolation overestimates  $R_f(\lambda)$  somewhat, particularly if the front side is planar. Typically this error results in an overestimation of  $R_f$  and underestimation of escape light by around 0.1-0.2 mA/cm<sup>2</sup> for planar surfaces, as found by comparison with ray-tracing simulations using the software package TracePro [16].

We divide the absorption spectra by  $(1 - R_f(\lambda))$  to correct for the effect of  $R_f(\lambda)$  on absorption. These corrected spectra are here marked with prime symbols '. The corrected Ag plateau value,  $A'_{plat}$ , which is a scalar value, is defined as:

$$A'_{plat} = \text{mean} \left( \frac{A_{meas}(\lambda=1250-1300 \text{ nm})}{1-R_f(\lambda=1250-1300 \text{ nm})} \right) \quad (1)$$

The Si absorption,  $A'_{Si}(\lambda)$ , can now be found as follows:

$$A'_{Si}(\lambda) = \frac{A'_{meas}(\lambda) - A'_{plat}}{1 - A'_{plat}} \quad (2)$$

Our samples are moderately doped (1-3  $\Omega\text{cm}$ , p-type) so we ignore the contribution of free carrier absorption. The light that is not absorbed in the Si is assumed to be Ag absorption,  $A'_{Ag}(\lambda)$ :

$$A'_{Ag}(\lambda) = A'_{meas}(\lambda) - A'_{Si}(\lambda) \quad (3)$$

To get the non-primed absorption values, we simply multiply the primed values with  $(1 - R_f(\lambda))$ .

The optical losses related to front side reflectance and parasitic absorption can be calculated from  $R_f(\lambda)$  and  $A_{Ag}(\lambda)$ . In addition we may extract the escape loss,  $R_{esc}(\lambda)$ :

$$R_{esc}(\lambda) = R_{meas}(\lambda) - R_f(\lambda) \quad (4)$$

To test the procedure described in this section we apply it to ray-tracing simulations. The simulations allow the extraction of wavelength dependent Si absorption, Ag absorption and front side reflection. We simulate a planar structure, a structure with a Lambertian reflector with 99 % reflectivity and a double-side pyramidal structure [17]. From reflectance curves, the Ag absorption plateau is extracted. Ag and Si absorption determined by the method described above agree well with Ag and Si absorption registered by the ray-tracing program for all test structures. An example is shown in Fig. 3, where the estimated and simulated Si and Ag absorption is shown, for a Lambertian rear reflector with 99 % reflectivity.

The magnitude of the escape light will be dependent on the thickness of the cell and the wavelength integration limit. Rather than integrating to a fixed wavelength, e.g. 1.2  $\mu\text{m}$ ,

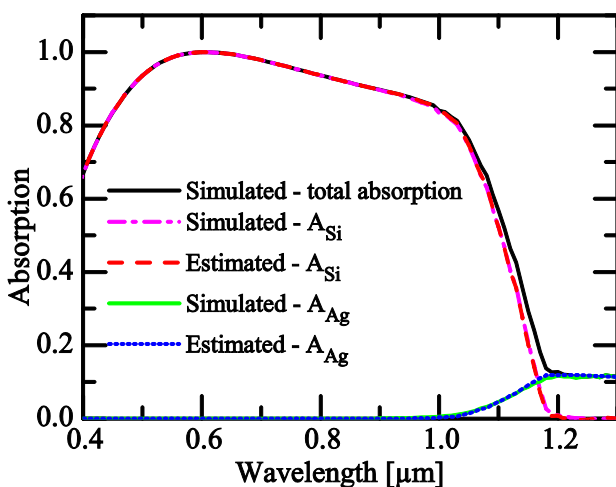


Fig. 3. Correspondence between simulated and estimated absorption for a 90  $\mu\text{m}$  thick wafer with a Lambertian rear reflector with 99 % reflectivity.

which would overestimate losses for thin cells, we weight the optical loss with the probability of absorption in a Lambertian cell of the same thickness, being a relevant reference for light trapping schemes. We do the same for the front side reflectance and the parasitic absorption. Fig. 4 shows measured absorption, Si absorption and the various optical losses in a 28  $\mu\text{m}$  thick sample with rear side dimples, as extracted using the method described above. We see that  $R_f$  contributes both at short and long wavelengths, whereas  $R_{esc}$  and  $A_{Ag}$  only contributes at long wavelengths where long optical absorption lengths allow the light to reach the rear surface and potentially to escape through the front of the wafer.

In order to quantify the optical properties in terms of current density or current density loss, the spectral properties are weighted against the AM1.5 solar spectrum. From the silicon absorption  $A_{Si}$ , we extract the photogenerated current density  $J_{ph}$ . Correspondingly, we extract the equivalent current losses from the various loss mechanisms. From  $R_f$ , we extract the primary reflectance loss  $J_{refl}$ , from  $R_{esc}$ , the escape light loss  $J_{esc}$  and from  $A_{Ag}$ , the loss from parasitic absorption  $J_{parasitic}$ .

### III. RESULTS

#### A. Texturing process

Fig. 5 (d) shows a SEM image of a part of one laser spot. We see a fairly homogenous processing result, with defects at imperfections in the microsphere crystal. The crystal is polycrystalline. We also see the edge between two adjacent laser spots as a line to the right. Here, the intensity is high enough for removal of the microspheres, but not high enough to penetrate the  $\text{SiN}_x$  etch barrier. Hence, the pattern will not form here. Some larger unprocessed areas are also observed (not shown here), where the microspheres have formed multilayer structures rather than monolayer structures.

When the texture is illuminated by a white-light source, a circular diffraction pattern is observed (Fig. 5 (e)). The circular pattern is an indication that we do not have any

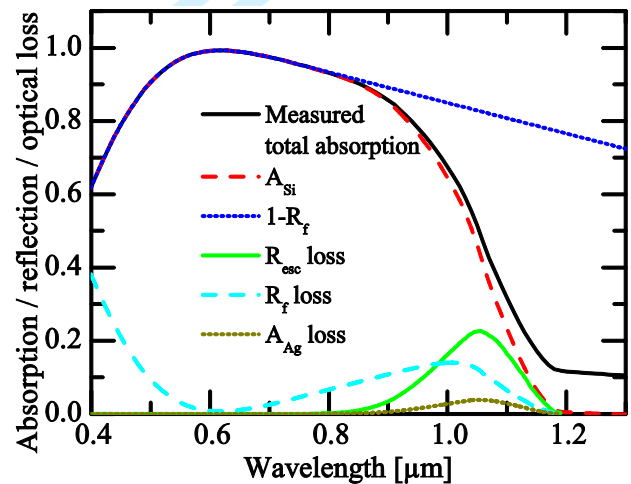


Fig. 4. Optical losses for a 28  $\mu\text{m}$  thick cell with planar front side and dimples on the rear side. The losses are weighted with the probability of absorption in a Lambertian wafer of equal thickness, seen as a cutoff of the absorption contributions towards 1.2  $\mu\text{m}$ .

> REPLACE THIS LINE WITH YOUR PAPER IDENTIFICATION NUMBER (DOUBLE-CLICK HERE TO EDIT) <

4

prevailing crystal orientation, as is also obvious from the SEM-image. The rainbow colors imply a wavelength dependence of the scattering angle, indicating that the structure is indeed diffractive, and not simply diffuse. This means that although the crystal grains are randomly oriented, the average neighbor to neighbor distances are well defined and is dominating the scattering properties.

Also shown in Fig. 5 are SEM-images of our reference textures; random pyramids (a), 70 seconds isotropic etch (b) and 180 seconds isotropic etch (c). The lines from the sawing process are clearly visible for the isotropic etches, and barely visible for the random pyramid etch. Note also how the appearance of the isotropic etch changes from the 70 seconds etch to the 180 seconds etch.

### B. Optical properties of the samples

The optical properties of the samples are analyzed and the results are summarized in Fig. 6. The photogenerated current,  $J_{ph}$ , is shown in Fig. 6(a). We observe that the samples with front side structures generate more current than the rear side structures, a difference of about  $2 \text{ mA/cm}^2$ . The samples with detached reflectors generate slightly more current than the ones with evaporated reflectors. Furthermore, we observe that the dimple structures generate more current than the planar reference, but less than the pyramidal structures. We shall analyze the contributions to this behavior in more detail.

Thicker wafers generally absorb more light than the thin wafers, causing increased  $J_{ph}$ , however trends caused by thickness are reduced in the graphs showing optical loss, as

the contributions are weighted against the Lambertian absorption at the given thickness as described in section II.B.

### C. Primary reflectance

Fig. 6(b) shows the primary reflectance loss,  $J_{refl}$ . It is around  $2 \text{ mA/cm}^2$  higher for the rear side textures, i.e. the textures with a planar front surface, compared to the front side textures, explaining the majority of the observed differences in photogenerated current. Textured front surfaces will allow for the light to experience multiple bounces at the wafer surface, increasing the transmission into the wafer. We observe that the random pyramids have a lower  $J_{refl}$  than the dimples. The random pyramids texture has steep angles ( $54.7^\circ$ ). This ensures multiple bounces for all of the incident light, and hence low primary reflectance. The dimples on the other hand have a lower  $J_{refl}$  than the isotropic textures.

It is important to note that the differences in  $J_{refl}$  will be lower when the cell is encapsulated under module glass and laminate, making this contribution less dominant. We have performed experiments on random pyramid textures and isotropic etched samples showing that a difference in  $J_{refl}$  of  $2.3 \text{ mA/cm}^2$  in air is reduced to only  $0.6 \text{ mA/cm}^2$  after encapsulation [18].

### D. Escape light

The escape light loss,  $J_{esc}$ , (Fig. 6(c)) for the planar reference is very high, indicating the lack of light trapping in this sample. On the other hand, the pyramidal structures have slightly lower  $J_{esc}$  than the dimples, indicating that this texture

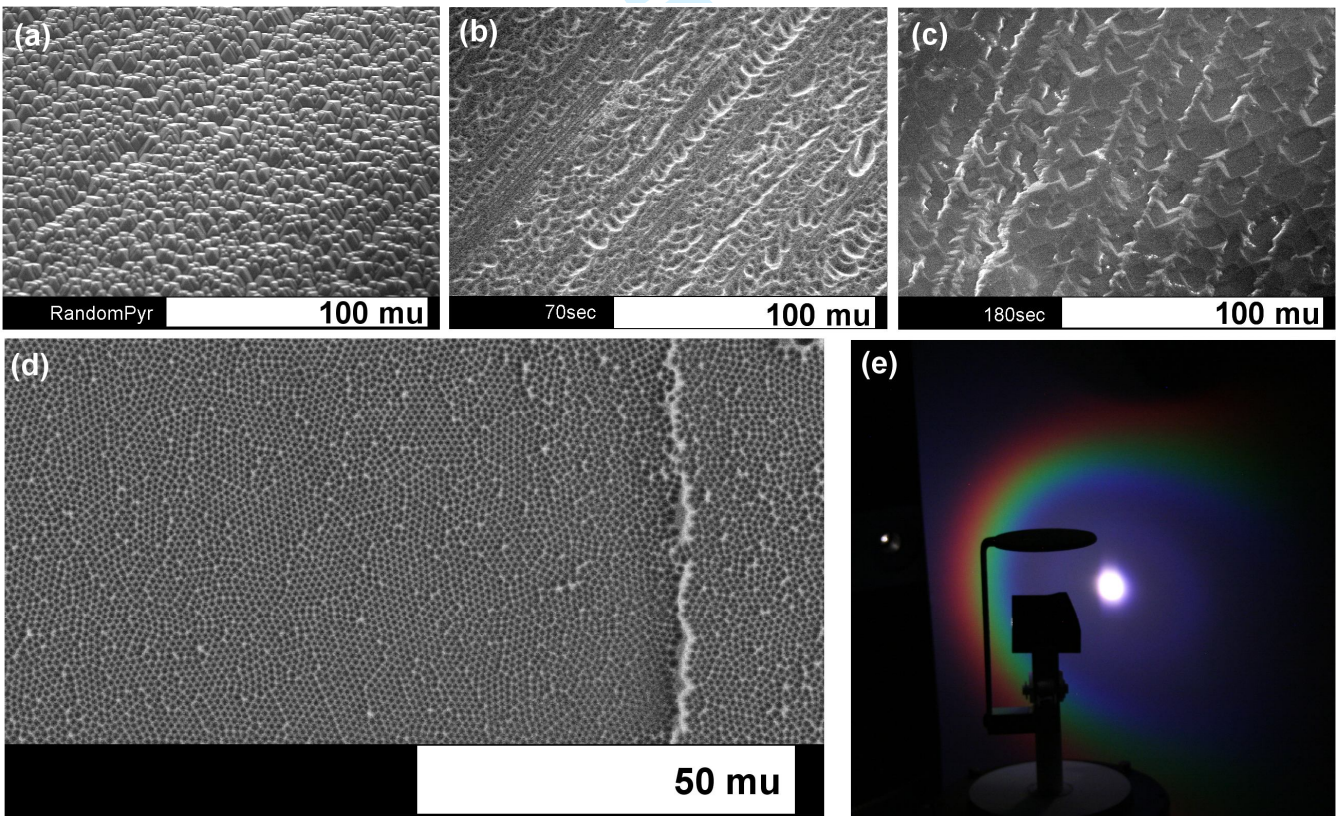


Fig. 5. Images of (a) the random pyramid, (b) the 70 second isotropic and (c) 180 second isotropic etches. (d) Dimple pattern in silicon, showing part of one laser spot. A homogenous processing result is seen, with minor defects caused by irregularities in the microsphere layer and at the edge of the laser spot. (e) Diffraction pattern from the texture when illuminated by a white-light source.

traps the light very efficiently. The scatter in the measurements on the dimples may be indicative of a slight inhomogeneity in the texture. We see that the use of front and rear side dimples result in the same  $J_{esc}$ , indicating that the light trapping properties of the texture is similar whether the texture is on the front or rear surface. Surprisingly, also the 70 seconds isotropic etched sample shows low  $J_{esc}$ , while showing fairly high primary reflectance loss. This behavior is indicative of the fact that multiple front-surface bounces requires quite steep front surface angles, which are not dominant for the isotropic etch, while fairly shallow rear surface angles is enough for the light reflected from the rear surface to hit the front surface at angles outside of the escape cone of silicon.

### E. Parasitic absorption

We observe that all structures with detached rear reflectors show very low  $J_{parasitic}$  (Fig. 6(d)). The evaporated reflectors, on the other hand have higher  $J_{parasitic}$ , indicating a stronger coupling to the rear reflector in this case. For the case of rear dimples with evaporated reflector, we see a significant increase in  $J_{parasitic}$ . This trend is not as strong for non-diffractive samples, indicating that microscopic periodicity is

required for increased parasitic absorption, as investigated by Springer *et al.* [13]. We also seem to experience an increase in  $J_{parasitic}$  for the thinnest cells, where a larger fraction of the incoming light will reach the rear reflector.

Silver is a material with high reflectivity, minimizing the impact of parasitic absorption. Using e.g. screen-printed aluminum, which has a much lower reflectivity, would certainly be detrimental to the rear-structured samples, increasing  $J_{parasitic}$ . On the other hand, the process proposed by Hauser *et al.* [10] may yield a planar dielectric on micro-textured surfaces, reducing  $J_{parasitic}$  for rear structured samples.

## IV. DISCUSSION

A more industrially oriented processing method could, instead of spin-coating the microspheres onto individual wafers, apply a microlens-array on a carrier [19]. Such an array could be re-used, simplifying the process. Using 400x400  $\mu\text{m}$  laser spots and 100 kHz pulse repetition rate, a 5 inch wafer can be processed in one second. Such laser parameters are industrially available. Furthermore, using an etch barrier which does not require vacuum deposition would significantly simplify the process. Laser damage to the wafer has been measured on other samples using similar laser

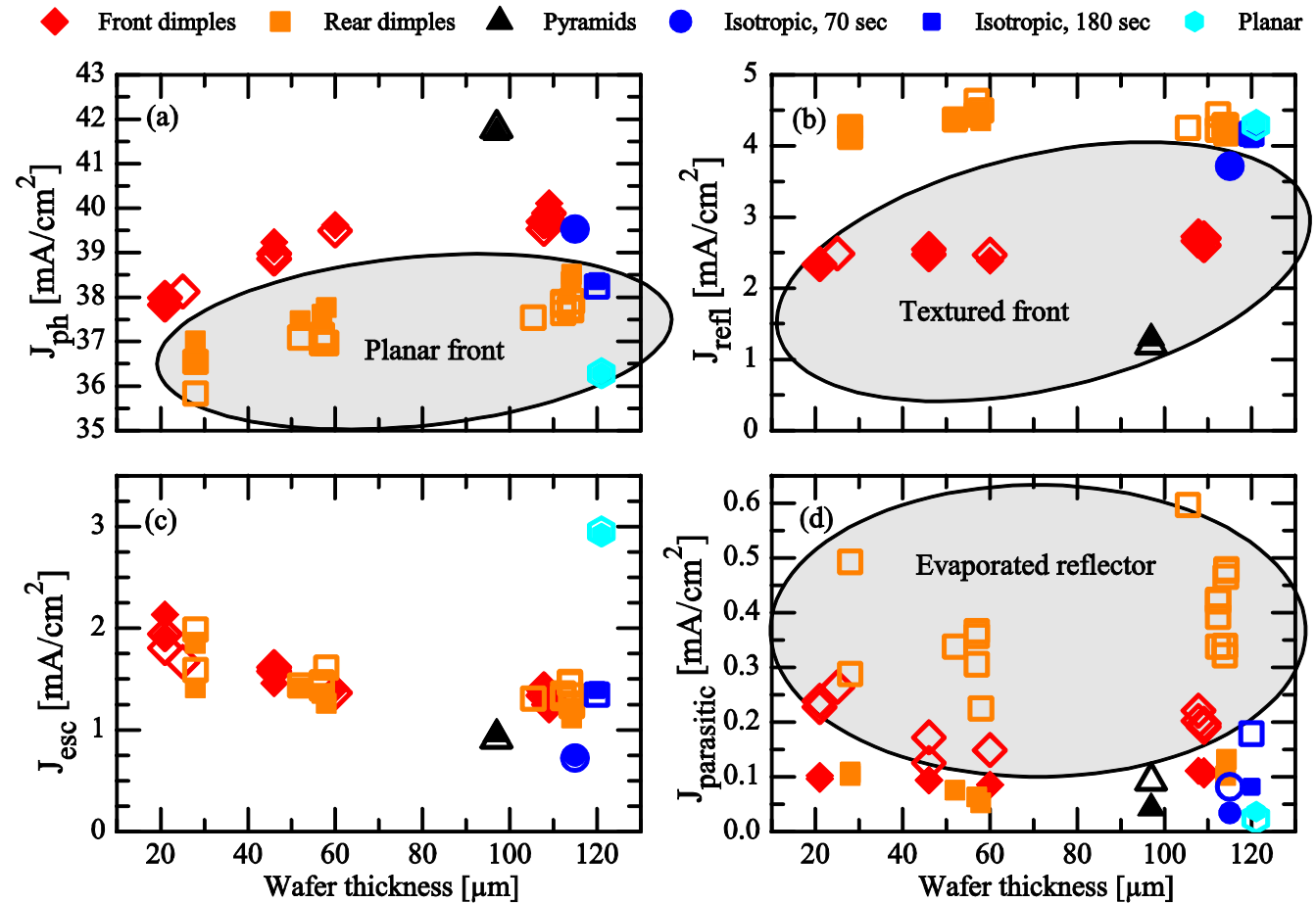


Fig. 6. Extracted optical performance of the textures. Filled symbols indicate detached rear reflector, whereas open symbols indicate evaporated rear reflector. Gray areas indicate the dominating behavior of a group of textures. Several trends are clear: Rear side textures have lower photogenerated current, mainly caused by higher primary reflectance. Evaporated reflectors cause higher parasitic absorption, especially for rear side textures. Pyramidal structures show higher photogenerated current than the dimple structures, mainly as a result of very low primary reflectance. Images of the random pyramid, 70 second isotropic and 180 second isotropic etches.

parameters, where etching of 0.27  $\mu\text{m}$  from the surface completely restored bulk lifetime. As such, we do not expect laser damage to be detrimental to this texture when applying ultrashort laser pulses.

Random pyramid and isotropic etches are dependent on proper seeding for good quality textures. We have observed a lowering of texture quality when moving from slurry to diamond wire cut wafers. With certain kerf-less wafering technologies, proper seeding of the etch structures will be a challenge, and the performance of an isotropic texture would be hampered compared to our texture, which does not require any additional seeding. The two different isotropic etched samples are meant to illustrate different states of surface roughness. We see that the more polished 180 seconds sample delivers significantly lower  $J_{ph}$  than the 70 seconds sample. As our 100  $\mu\text{m}$  thick dimple structures deliver roughly the same  $J_{ph}$  as the 70 seconds isotropic etched samples from diamond cut wafers, we have reason to believe that our structures will outperform isotropic etched textures on wafers from certain kerf-less technologies. In addition, the isotropic etch removes several micrometers from each side of the wafer. As such, the dimple structure is more suitable for thin silicon wafers.

The fact that our texture is a single sided texture may be beneficial, potentially simplifying laser processing (e.g. for local contact openings) on the planar side of the wafer [20] and reducing surface recombination.

Microscope images (not shown here) have shown that samples with dimple structures have to different degrees areas that are not textured. Such areas will naturally not contribute to light trapping or lower reflection. It is therefore viable that even better light trapping might be achieved by improving the monolayer fill factor. Improvement of the crystallinity of the texture may also alter the light-trapping properties.

## V. CONCLUSION

We have fabricated thin silicon solar cells with a diffractive structure based on a hexagonally ordered dimple pattern, and experimentally compared the light-trapping properties of our structures with a random pyramid texture, isotropic textures and planar references. We see that applying the texture to the front surface is far more efficient than applying it to the rear surface, as a result of lower front reflectance combined with lower parasitic absorption. The performance of our dimple structures lies between that of the planar and random pyramid textures, being roughly similar to the 70 seconds isotropic etched structures.

The main sources of loss compared to the random pyramid texture are front surface reflectance, a contribution which will be significantly lower when the cell is incorporated in a module, and parasitic absorption, especially in the cases where a micro-structured rear reflector is used.

The main benefit of our structure is that it is suitable for very thin wafers and wafers without saw damage, and that the etching process does not cause significant thinning of the wafer. Further improvement of the performance of the texture may be obtained through higher area coverage and better crystal quality of the texture, and by improving the

hemispherical shape of the dimples.

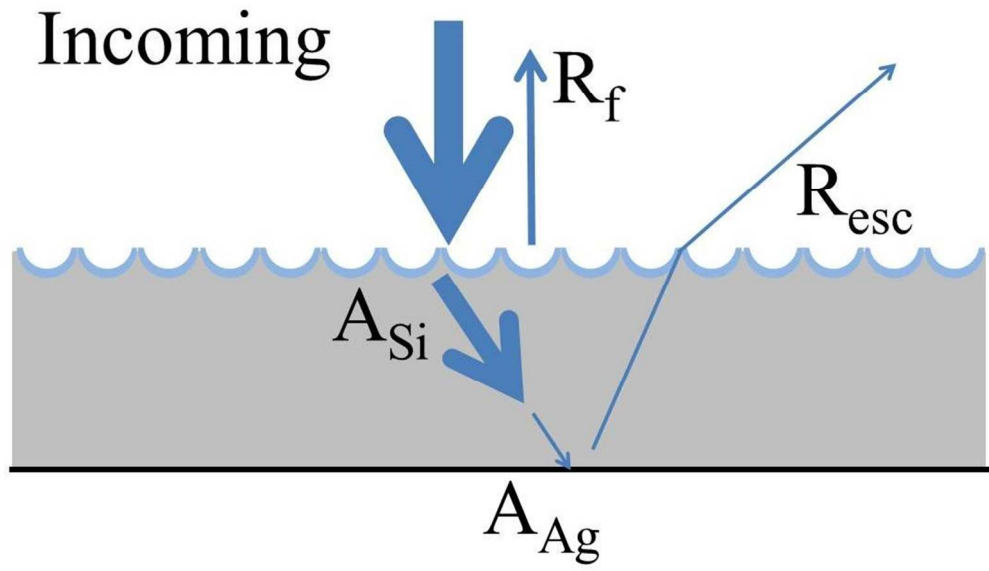
## ACKNOWLEDGMENT

The authors gratefully acknowledge the input received from Prof. Aasmund Sudbø (University of Oslo) in forming the contents of this article.

## REFERENCES

- [1] K. Branker, M. J. M. Pathak, and J. M. Pearce, "A review of solar photovoltaic leveled cost of electricity," *Renew. Sust. Energ. Rev.*, vol. 15, no. 9, pp. 4470–4482, Dec. 2011.
- [2] F. Henley, S. Kang, Z. Liu, L. Tian, J. Wang, and Y.-L. Chow, "Beam-induced wafering technology for kerf-free thin PV manufacturing," in *Proc. 34th IEEE Photovolt. Spec. Conf.*, Philadelphia, PA, 2009, pp. 001718–001723.
- [3] M. Ernst and R. Brendel, "Layer transfer of large area macroporous silicon for monocrystalline thin-film solar cells," in *Proc. 35th IEEE Photovolt. Spec. Conf.*, Honolulu, HI, 2010, pp. 003122–003124.
- [4] R. A. Rao, L. Mathew, S. Saha, S. Smith, D. Sarkar, R. Garcia, R. Stout, A. Gurmu, E. Onyegam, D. Ahn, D. Xu, D. Jawarani, J. Fossum, and S. Banerjee, "A novel low cost 25 $\mu\text{m}$  thin exfoliated monocrystalline Si solar cell technology," in *Proc. 37th IEEE Photovolt. Spec. Conf.*, Seattle, WA, 2011, pp. 001504–001507.
- [5] P. Rosenits, F. Kopp, and S. Reber, "Epitaxially grown crystalline silicon thin-film solar cells reaching 16.5% efficiency with basic cell process," *Thin Solid Films*, vol. 519, no. 10, pp. 3288–3290, Mar. 2011.
- [6] J. Cichoszewski, M. Reuter, and J. H. Werner, "+0.4% Efficiency gain by novel texture for String Ribbon solar cells," *Sol. Energ. Mat. Sol. Cells*, vol. 101, pp. 1–4, Jun. 2012.
- [7] J. Gjessing, A. S. Sudbø, and E. S. Marstein, "Comparison of periodic light-trapping structures in thin crystalline silicon solar cells," *J. Appl. Phys.*, vol. 110, no. 3, p. 033104, 2011.
- [8] A. Gombert, K. Rose, A. Heinzl, W. Horbelt, C. Zanke, B. Bläsi, and V. Wittwer, "Antireflective submicrometer surface-relief gratings for solar applications," *Sol. Energ. Mat. Sol. Cells*, vol. 54, pp. 333–342, Jul. 1998.
- [9] S. H. Zaidi, J. M. Gee, and D. S. Ruby, "Diffraction grating structures in solar cells," in *Proc. 28th IEEE Photovolt. Spec. Conf.*, Anchorage, AK, 2000, pp. 395–398.
- [10] H. Hauser, B. Michl, V. Kübler, S. Schwarzkopf, C. Müller, M. Hermle, and B. Bläsi, "Nanoimprint Lithography for Honeycomb Texturing of Multicrystalline Silicon," *Energy Procedia*, vol. 8, pp. 648–653, 2011.
- [11] H. Hauser, A. Mellor, A. Guttowski, C. Wellens, J. Benick, C. Müller, M. Hermle, and B. Bläsi, "Diffractive Backside Structures via Nanoimprint Lithography," *Energy Procedia*, vol. 27, pp. 337–342, 2012.
- [12] J. Thorstensen, J. Gjessing, E. Haugan, and S. E. Foss, "2D periodic gratings by laser processing," *Energy Procedia*, vol. 27, pp. 343–348, 2012.
- [13] J. Springer, A. Poruba, L. Müllerova, M. Vanecek, O. Kluth, and B. Rech, "Absorption loss at nanorough silver back reflector of thin-film silicon solar cells," *J. Appl. Phys.*, vol. 95, no. 3, pp. 1427–1429, 2004.
- [14] E. Haugan, H. Granlund, J. Gjessing, and E. S. Marstein, "Colloidal Crystals as Templates for Light Harvesting Structures in Solar Cells," *Energy Procedia*, vol. 10, pp. 292–296, 2011.
- [15] J. Gjessing, E. S. Marstein, and A. Sudbø, "2D back-side diffraction grating for improved light trapping in thin silicon solar cells.," *Opt. express*, vol. 18, no. 6, pp. 5481–95, Mar. 2010.
- [16] "TracePro". <http://www.lambdare.com>, 2012.
- [17] J. Gjessing, E. S. Marstein, and A. S. Sudbø, "Comparison of light trapping in diffractive and random pyramidal structures," in *Proc. 26th Eur. Photovolt. Solar Energy Conf.*, Hamburg, Germany, 2011, pp. 2759–2763.
- [18] J. Gjessing, "To be published".
- [19] R. Denk, K. Piglmayer, and D. Bäuerle, "Laser-induced nano-patterning by means of interference subpatterns generated by microspheres," *Appl. Phys. A Mater. Sci. Process.*, vol. 76, no. 1, pp. 1–3, Jan. 2003.
- [20] S. Hermann, T. Dezhdar, N.-P. Harder, R. Brendel, M. Seibt, and S. Stroj, "Impact of surface topography and laser pulse duration for laser ablation of solar cell front side passivating SiNx layers", *J. Appl. Phys.*, vol. 108, no. 11, p. 114514, 2010.

1  
2  
3  
4  
5  
6  
7  
8  
9  
10  
11  
12  
13  
14  
15  
16  
17  
18  
19  
20  
21  
22  
23  
24  
25  
26  
27  
28  
29  
30  
31  
32  
33  
34  
35  
36  
37  
38  
39  
40  
41  
42  
43  
44  
45  
46  
47  
48  
49  
50  
51  
52  
53  
54  
55  
56  
57  
58  
59  
60



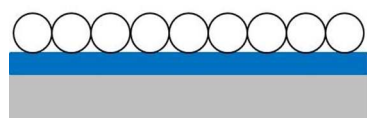
379x218mm (72 x 72 DPI)

view Only

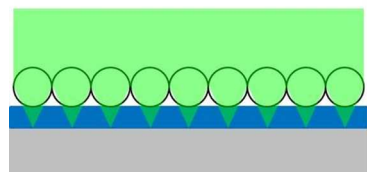
1  
2  
3  
4  
5  
6  
7  
8  
9  
10  
11  
12  
13  
14  
15  
16  
17  
18  
19  
20  
21  
22  
23  
24  
25  
26  
27  
28  
29  
30  
31  
32  
33  
34  
35  
36  
37  
38  
39  
40  
41  
42  
43  
44  
45  
46  
47  
48  
49  
50  
51  
52  
53  
54  
55  
56  
57  
58  
59  
60



SiN<sub>x</sub> etch barrier deposition



Microsphere deposition



Laser irradiation



Openings through etch barrier



Etching

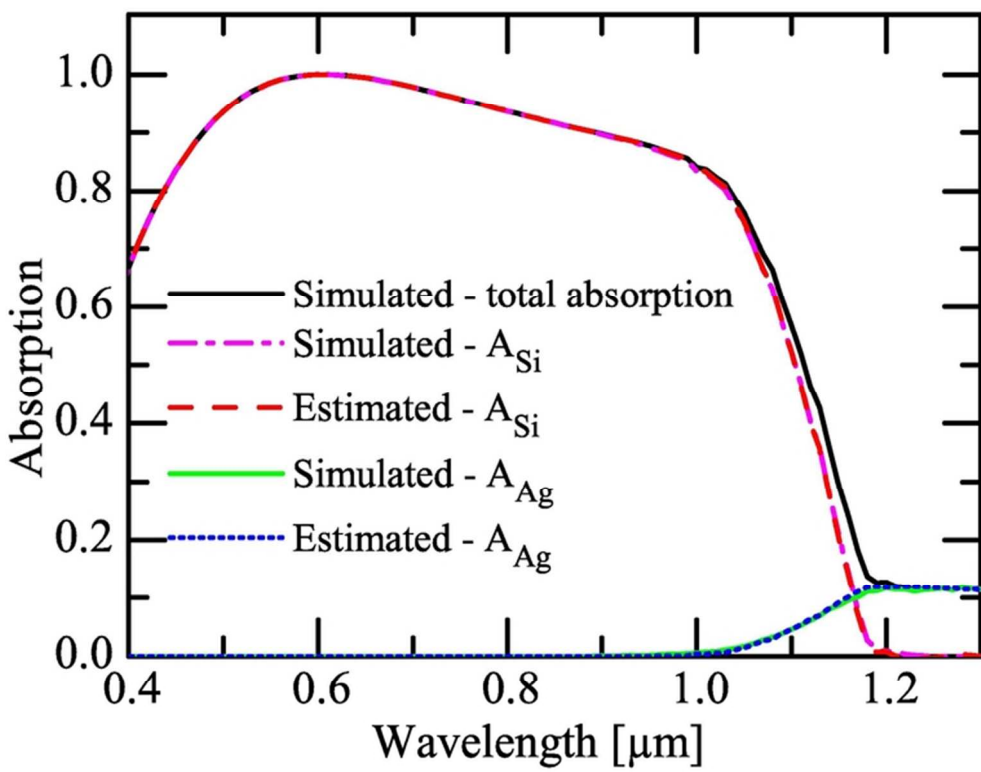


Finished structure (front / rear)

216x172mm (150 x 150 DPI)

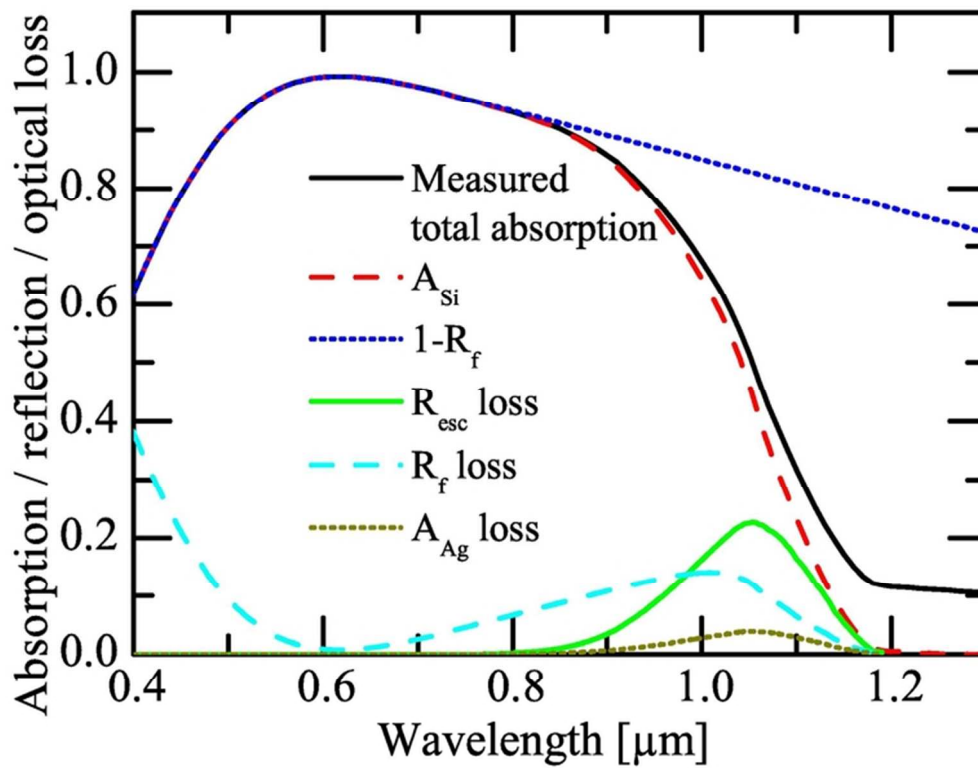
Only

1  
2  
3  
4  
5  
6  
7  
8  
9  
10  
11  
12  
13  
14  
15  
16  
17  
18  
19  
20  
21  
22  
23  
24  
25  
26  
27  
28  
29  
30  
31  
32  
33  
34  
35  
36  
37  
38  
39  
40  
41  
42  
43  
44  
45  
46  
47  
48  
49  
50  
51  
52  
53  
54  
55  
56  
57  
58  
59  
60



65x50mm (300 x 300 DPI)

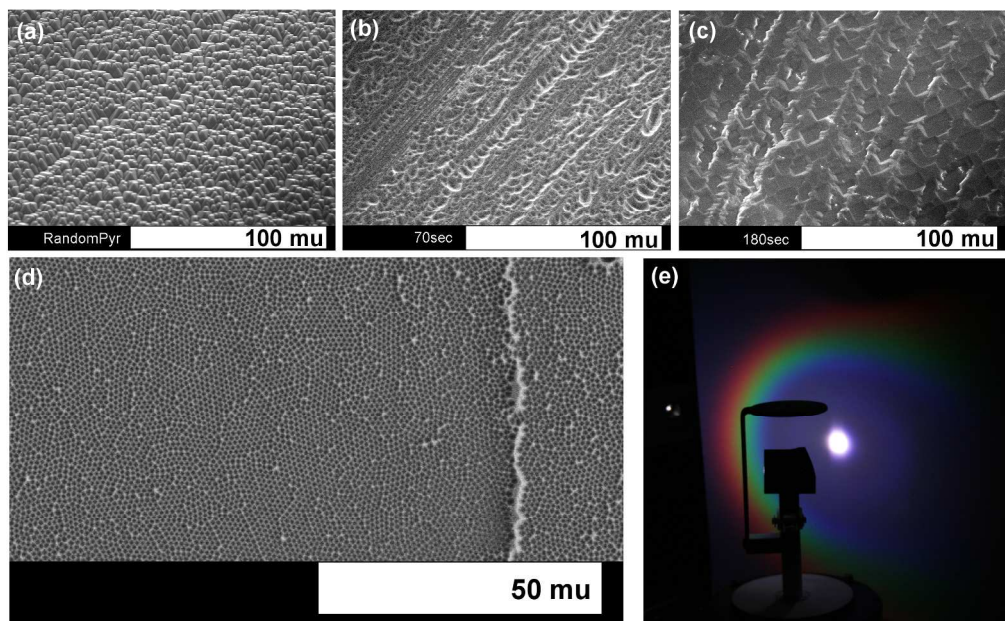
Only



65x50mm (300 x 300 DPI)

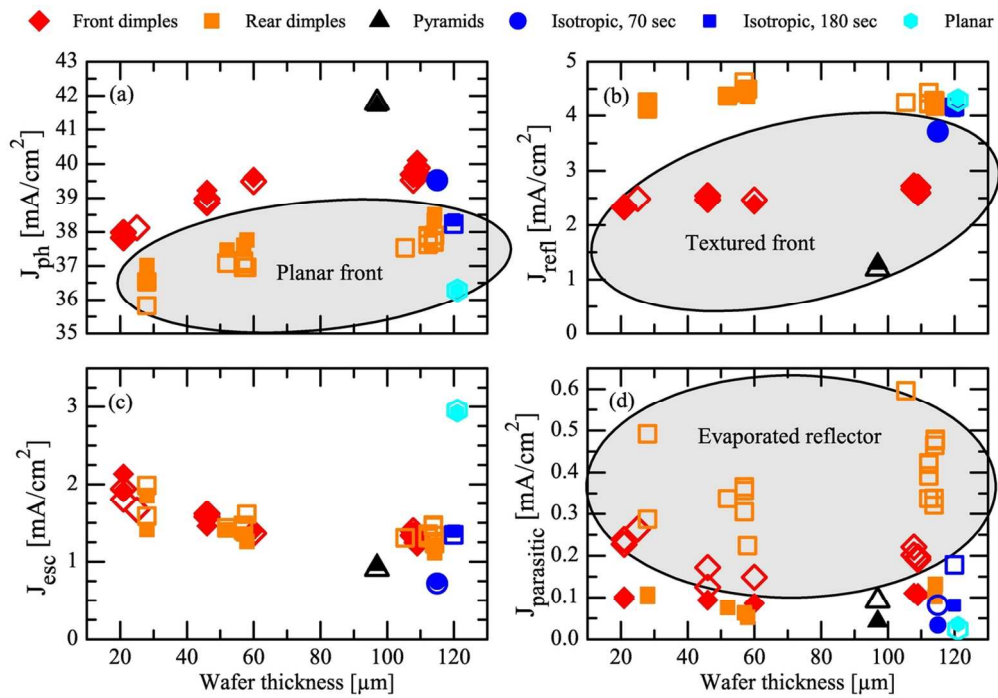
Only

1  
2  
3  
4  
5  
6  
7  
8  
9  
10  
11  
12  
13  
14  
15  
16  
17  
18  
19  
20  
21  
22  
23  
24  
25  
26  
27  
28  
29  
30  
31  
32  
33  
34  
35  
36  
37  
38  
39  
40  
41  
42  
43  
44  
45  
46  
47  
48  
49  
50  
51  
52  
53  
54  
55  
56  
57  
58  
59  
60



917x561mm (72 x 72 DPI)

View Only



117x81mm (300 x 300 DPI)

Only

1  
 2  
 3  
 4  
 5  
 6  
 7  
 8  
 9  
 10  
 11  
 12  
 13  
 14  
 15  
 16  
 17  
 18  
 19  
 20  
 21  
 22  
 23  
 24  
 25  
 26  
 27  
 28  
 29  
 30  
 31  
 32  
 33  
 34  
 35  
 36  
 37  
 38  
 39  
 40  
 41  
 42  
 43  
 44  
 45  
 46  
 47  
 48  
 49  
 50  
 51  
 52  
 53  
 54  
 55  
 56  
 57  
 58  
 59  
 60

### IEEE COPYRIGHT AND CONSENT FORM

To ensure uniformity of treatment among all contributors, other forms may not be substituted for this form, nor may any wording of the form be changed. This form is intended for original material submitted to the IEEE and must accompany any such material in order to be published by the IEEE. Please read the form carefully and keep a copy for your files.

**TITLE OF PAPER/ARTICLE/REPORT, INCLUDING ALL CONTENT IN ANY FORM, FORMAT, OR MEDIA (hereinafter, "the Work"):**

*Light-trapping properties of a diffractive honeycomb structure in Silicon*

**COMPLETE LIST OF AUTHORS:**

*Jostein Thorstensen, Jo Gjessing, Erik Stensrud Marstein, Sean Erik Foss*

**IEEE PUBLICATION TITLE (Journal, Magazine, Conference, Book):**

*Journal of Photovoltaics*

#### COPYRIGHT TRANSFER

1. The undersigned hereby assigns to The Institute of Electrical and Electronics Engineers, Incorporated (the "IEEE") all rights under copyright that may exist in and to: (a) the above Work, including any revised or expanded derivative works submitted to the IEEE by the undersigned based on the Work; and (b) any associated written or multimedia components or other enhancements accompanying the Work.

#### CONSENT AND RELEASE

2. In the event the undersigned makes a presentation based upon the Work at a conference hosted or sponsored in whole or in part by the IEEE, the undersigned, in consideration for his/her participation in the conference, hereby grants the IEEE the unlimited, worldwide, irrevocable permission to use, distribute, publish, license, exhibit, record, digitize, broadcast, reproduce and archive, in any format or medium, whether now known or hereafter developed: (a) his/her presentation and comments at the conference; (b) any written materials or multimedia files used in connection with his/her presentation; and (c) any recorded interviews of him/her (collectively, the "Presentation"). The permission granted includes the transcription and reproduction of the Presentation for inclusion in products sold or distributed by IEEE and live or recorded broadcast of the Presentation during or after the conference.

3. In connection with the permission granted in Section 2, the undersigned hereby grants IEEE the unlimited, worldwide, irrevocable right to use his/her name, picture, likeness, voice and biographical information as part of the advertisement, distribution and sale of products incorporating the Work or Presentation, and releases IEEE from any claim based on right of privacy or publicity.

4. The undersigned hereby warrants that the Work and Presentation (collectively, the "Materials") are original and that he/she is the author of the Materials. To the extent the Materials incorporate text passages, figures, data or other material from the works of others, the undersigned has obtained any necessary permissions. Where necessary, the undersigned has obtained all third party permissions and consents to grant the license above and has provided copies of such permissions and consents to IEEE.

Please check this box if you do not wish to have video/audio recordings made of your conference presentation.  
See reverse side for Retained Rights/Terms and Conditions, and Author Responsibilities.

#### GENERAL TERMS

- The undersigned represents that he/she has the power and authority to make and execute this assignment.
- The undersigned agrees to indemnify and hold harmless the IEEE from any damage or expense that may arise in the event of a breach of any of the warranties set forth above.
- In the event the above work is not accepted and published by the IEEE or is withdrawn by the author(s) before acceptance by the IEEE, the foregoing copyright transfer shall become null and void and all materials embodying the Work submitted to the IEEE will be destroyed.
- For jointly authored Works, all joint authors should sign, or one of the authors should sign as authorized agent for the others.

(1) *Jostein Thorstensen*  
Author/Authorized Agent for Joint Authors

*11. Nov. 2012, Kjeller, Norway*  
Date

#### U.S. GOVERNMENT EMPLOYEE CERTIFICATION (WHERE APPLICABLE)

This will certify that all authors of the Work are U.S. government employees and prepared the Work on a subject within the scope of their official duties. As such, the Work is not subject to U.S. copyright protection.

(2) \_\_\_\_\_  
Authorized Signature

\_\_\_\_\_  
Date

(Authors who are U.S. government employees should also sign signature line (1) above to enable the IEEE to claim and protect its copyright in international jurisdictions.)

#### CROWN COPYRIGHT CERTIFICATION (WHERE APPLICABLE)

This will certify that all authors of the Work are employees of the British or British Commonwealth Government and prepared the Work in connection with their official duties. As such, the Work is subject to Crown Copyright and is not assigned to the IEEE as set forth in the first sentence of the Copyright Transfer Section above. The undersigned acknowledges, however, that the IEEE has the right to publish, distribute and reprint the Work in all forms and media.

(3) \_\_\_\_\_  
Authorized Signature

\_\_\_\_\_  
Date

(Authors who are British or British Commonwealth Government employees should also sign line (1) above to indicate their acceptance of all terms other than the copyright transfer.)

1  
2  
3  
4  
5  
6  
7  
8  
9

## IEEE COPYRIGHT FORM *(continued)*

### RETAINED RIGHTS/TERMS AND CONDITIONS

#### General

- 10 1. Authors/employers retain all proprietary rights in any process, procedure, or article of manufacture described in the Work.  
 11 2. Authors/employers may reproduce or authorize others to reproduce the Work, material extracted verbatim from the Work, or derivative works for the  
 12 author's personal use or for company use, provided that the source and the IEEE copyright notice are indicated, the copies are not used in any way that  
 13 implies IEEE endorsement of a product or service of any employer, and the copies themselves are not offered for sale.  
 14 3. In the case of a Work performed under a U.S. Government contract or grant, the IEEE recognizes that the U.S. Government has royalty-free  
 15 permission to reproduce all or portions of the Work, and to authorize others to do so, for official U.S. Government purposes only, if the contract/grant  
 16 so requires.  
 17 4. Although authors are permitted to re-use all or portions of the Work in other works, this does not include granting third-party requests for reprinting,  
 18 republishing, or other types of re-use. The IEEE Intellectual Property Rights office must handle all such third-party requests.  
 19 5. Authors whose work was performed under a grant from a government funding agency are free to fulfill any deposit mandates from that funding  
 20 agency.

#### Author Online Use

- 21  
 22 6. **Personal Servers.** Authors and/or their employers shall have the right to post the accepted version of IEEE-copyrighted articles on their own  
 23 personal servers or the servers of their institutions or employers without permission from IEEE, provided that the posted version includes a prominently  
 24 displayed IEEE copyright notice and, when published, a full citation to the original IEEE publication, including a link to the article abstract in IEEE  
 25 Xplore. Authors shall not post the final, published versions of their papers.  
 26 7. **Classroom or Internal Training Use.** An author is expressly permitted to post any portion of the accepted version of his/her own IEEE-  
 27 copyrighted articles on the author's personal web site or the servers of the author's institution or company in connection with the author's teaching,  
 28 training, or work responsibilities, provided that the appropriate copyright, credit, and reuse notices appear prominently with the posted material.  
 29 Examples of permitted uses are lecture materials, course packs, e-reserves, conference presentations, or in-house training courses.  
 30 8. **Electronic Preprints.** Before submitting an article to an IEEE publication, authors frequently post their manuscripts to their own web site, their  
 31 employer's site, or to another server that invites constructive comment from colleagues. Upon submission of an article to IEEE, an author is required to  
 32 transfer copyright in the article to IEEE, and the author must update any previously posted version of the article with a prominently displayed IEEE  
 33 copyright notice. Upon publication of an article by the IEEE, the author must replace any previously posted electronic versions of the article with either  
 34 (1) the full citation to the IEEE work with a Digital Object Identifier (DOI) or link to the article abstract in IEEE Xplore, or (2) the accepted version  
 35 only (not the IEEE-published version), including the IEEE copyright notice and full citation, with a link to the final, published article in IEEE Xplore.

### INFORMATION FOR AUTHORS

#### Author Responsibilities

36 The IEEE distributes its technical publications throughout the world and wants to ensure that the material submitted to its publications is properly  
 37 available to the readership of those publications. Authors must ensure that their Work meets the requirements as stated in section 8.2.1 of the IEEE  
 38 PSPB Operations Manual, including provisions covering originality, authorship, author responsibilities and author misconduct. More information on  
 39 IEEE's publishing policies may be found at [http://www.ieee.org/publications\\_standards/publications/rights/pub\\_tools\\_policies.html](http://www.ieee.org/publications_standards/publications/rights/pub_tools_policies.html). Authors are  
 40 advised especially of IEEE PSPB Operations Manual section 8.2.1.B12: "It is the responsibility of the authors, not the IEEE, to determine whether  
 41 disclosure of their material requires the prior consent of other parties and, if so, to obtain it." Authors are also advised of IEEE PSPB Operations  
 42 Manual section 8.1.1B: "Statements and opinions given in work published by the IEEE are the expression of the authors."

#### Author/Employer Rights

43 If you are employed and prepared the Work on a subject within the scope of your employment, the copyright in the Work belongs to your employer as  
 44 a work-for-hire. In that case, the IEEE assumes that when you sign this Form, you are authorized to do so by your employer and that your employer has  
 45 consented to the transfer of copyright, to the representation and warranty of publication rights, and to all other terms and conditions of this Form. If  
 46 such authorization and consent has not been given to you, an authorized representative of your employer should sign this Form as the Author.

#### IEEE Copyright Ownership

47 It is the formal policy of the IEEE to own the copyrights to all copyrightable material in its technical publications and to the individual contributions  
 48 contained therein, in order to protect the interests of the IEEE, its authors and their employers, and, at the same time, to facilitate the appropriate re-use  
 49 of this material by others. The IEEE distributes its technical publications throughout the world and does so by various means such as hard copy,  
 50 microfiche, microfilm, and electronic media. It also abstracts and may translate its publications, and articles contained therein, for inclusion in various  
 51 compendiums, collective works, databases and similar publications.  
 52  
 53  
 54  
 55  
 56  
 57  
 58  
 59  
 60

**THIS FORM MUST ACCOMPANY THE SUBMISSION OF THE AUTHOR'S MANUSCRIPT.**  
**Questions about the submission of the form or manuscript must be sent to the publication's editor.**  
**Please direct all questions about IEEE copyright policy to:**  
**IEEE Intellectual Property Rights Office, [copyrights@ieee.org](mailto:copyrights@ieee.org), +1-732-562-3966 (telephone)**